

Modelling Gas Networks with Compressors: A port-Hamiltonian Approach

Thomas Bendokat* Peter Benner*,[†]
Sara Grundel* Ashwin S. Nayak*

*Max Planck Institute for Dynamics of Complex Technical Systems, Magdeburg, Germany.

Email: bendokat@mpi-magdeburg.mpg.de, ORCID: 0000-0002-0671-6291

Email: benner@mpi-magdeburg.mpg.de, ORCID: 0000-0003-3362-4103

Email: grundel@mpi-magdeburg.mpg.de, ORCID: 0000-0002-0209-6566

Email: anayak@mpi-magdeburg.mpg.de, ORCID: 0000-0002-9855-2377

[†]Otto von Guericke University, Magdeburg, Germany.

Abstract: Transient gas network simulations can significantly assist in design and operational aspects of gas networks. Models used in these simulations require a detailed framework integrating various models of the network constituents - pipes and compressor stations among others. In this context, the port-Hamiltonian modelling framework provides an energy-based modelling approach with a port-based coupling mechanism. This study investigates developing compressor models in an integrated isothermal port-Hamiltonian model for gas networks. Four different models of compressors are considered and their inclusion in a larger network model is detailed. A numerical implementation for a simple testcase is provided to confirm the validity of the proposed model and to highlight their differences.

Keywords: gas networks, port-Hamiltonian system, compressor, mathematical modelling, numerical simulation

Mathematics subject classification: 93-10, 93-04, 76N15

Novelty statement:

- A first attempt at including compressors in port-Hamiltonian formulation for gas networks.
- Four nodal models for compressors with a pairwise combination of two specifications and two assumptions.
- Numerical implementation for a simple testcase.
- Publicly available software material for reproducibility and extension.

1 Introduction

Transportation of hydrogen is a vital strategy in Germany's renewable energy transition. The federal government has drawn up regulatory policies, convened gas transmission operators and has proposed developing a new core hydrogen-gas network alongside initiatives to repurpose existing pipeline infrastructure. The initiative brings forth a host of technical challenges related to an optimal design of a gas network and its operation [6, 14].

A gas transportation network comprises mainly of large pipelines interconnected at junctions, but there exist other critical components which can influence gas flow. Network design and operation

decisions can be aided by simulation tools that can predict the transmission operators with vital supply requirement for target demands within the network. The computational tools serve as an a priori analysis tool into the transient behavior of gas within the network and its components greatly improving efficiency and reliability. Gas networks crucially contain compressor stations specifically to increase the pressure of incoming gas stream, to compensate for pressure loss due to flow and friction in the pipes. A significant portion of the operational costs of gas networks are attributed to compressor stations and this differs vastly for hydrogen, natural gas and their blends [18]. A digital twin of the entire gas network can aid in such economic forecasts, redundancy planning and emergency response.

An accurate simulation of gas networks requires an integrated model of all its constituents. Network models have generally emphasized on connected pipeline flow models with only recent studies focusing on including compressor models [2, 8, 12, 17]. Typical models of compressor stations are based on their power ratings, whereas some models consider it as a node with the pressure scaled by a *compression ratio* [2, 8] or as an element scaling the in-flow to a specified *target pressure* [13]. In this study, an integrated model is proposed from an energy-based modelling viewpoint considering that gas networks fit into a port-Hamiltonian framework [4, 9–11, 13]. Port-Hamiltonian systems are a combination of port-based modeling and geometric mechanics and are well suited for modeling physical networks such as gas networks. An introduction and overview of these models can be found in [20]. Such models are suitable to be solved using geometric integration methods, preserving the structure. An emphasis in this study is placed specifically on including compressor models within the port-Hamiltonian models for gas networks and its software implementation.

2 Gas Networks

Gas networks consist of many components: pipes, compressors, resistances, heaters, coolers, valves, etc. [4]. In this study, we focus on the former two, combining them in a port-Hamiltonian fashion.

2.1 Pipe Model

As gas pipelines are long and thin, gas flow in a pipe can be modelled using the *Euler equations* in one spatial dimension [4, 12],

$$\begin{aligned}\partial_t \rho + \partial_x(\rho v) &= 0, \\ \partial_t(\rho v) + \partial_x(p + \rho v^2) &= -\frac{\lambda}{2D} \rho v |v| - g \rho \sin \alpha, \\ \partial_t E + \partial_x((E + p)v) &= -\frac{k_w}{D}(T - T_w),\end{aligned}\tag{1}$$

where ρ denotes the *density* of the gas, v denotes the *velocity*, p is the *pressure*, $E = \rho(\frac{1}{2}v^2 + c_v T + gh)$ is the *total energy* with *specific heat* c_v and *height* h , T is the *temperature* of the gas and T_w is the *temperature of the wall*. Furthermore, λ is the *pipe friction coefficient*, D is the *diameter* of the pipe, g the *gravitational constant*, α the *inclination angle* of the pipe and k_w the *heat transfer coefficient* of the wall. The pressure, density, and temperature are connected via the *equation of state*

$$p = \rho R T z(p, T),\tag{2}$$

with *gas constant* R and *compressibility factor* $z(p, T)$.

The Euler equations (1) can be transformed into port-Hamiltonian form as they are, but for our case we use the simplified ISO2b model [4], by making the following assumptions:

1. The model is *isothermal*, meaning the temperature of the pipe is constant in time and space.
2. The gas velocity v is insignificant compared to the (constant) speed of sound c , i.e., $(v/c)^2 \ll 1$.
3. The pressure in a pipe is related to the density by $p = c^2 \rho$.
4. The influence of gravity is neglected.

The ISO2b model then reads

$$\begin{aligned}\partial_t \rho + \partial_x m &= 0, \\ \partial_t m + \partial_x p &= -\frac{\lambda}{2D} m |v|,\end{aligned}\tag{3}$$

with *momentum* $m = \rho v$.

We apply the ISO2b model in port-Hamiltonian form to a pipe of length L , i.e., $x \in [0, L]$. To that end, define the *state* $\mathbf{z}(x, t) = \begin{bmatrix} \rho(x, t) \\ m(x, t) \end{bmatrix}$ and the *effort* $\mathbf{e}(\mathbf{z})(x, t) = \begin{bmatrix} p(\rho(x, t)) \\ m(x, t) \end{bmatrix}$, as well as

$$\mathbf{J}(\mathbf{z}) = \begin{bmatrix} 0 & -D_x \\ -D_x & 0 \end{bmatrix} \quad \text{and} \quad \mathbf{R}(\mathbf{z}) = \begin{bmatrix} 0 & 0 \\ 0 & \frac{\lambda}{2D} |v| \end{bmatrix},$$

where D_x is the differential operator $D_x f = f_x$ for any function $f: [0, L] \rightarrow \mathbb{R}$. Similar to [4], we can enforce the pressure p_0 at the inflow and the momentum m_L at the outflow of the pipe as boundary conditions, and write the ISO2b model in input-output port-Hamiltonian form as

$$\begin{aligned}\begin{bmatrix} I_2 \\ 0 \end{bmatrix} \dot{\mathbf{z}} &= \begin{bmatrix} \mathbf{J}(\mathbf{z}) - \mathbf{R}(\mathbf{z}) & 0 \\ -U & 0 \end{bmatrix} \begin{bmatrix} \mathbf{e}(\mathbf{z}) \\ Y\mathbf{e}(\mathbf{z}) \end{bmatrix} + \begin{bmatrix} 0 \\ I_2 \end{bmatrix} \mathbf{u} \\ \mathbf{y} &= \begin{bmatrix} 0 & I_2 \end{bmatrix} \begin{bmatrix} \mathbf{e}(\mathbf{z}) \\ Y\mathbf{e}(\mathbf{z}) \end{bmatrix},\end{aligned}\tag{4}$$

where

$$U\mathbf{e}(\mathbf{z}) = \begin{bmatrix} \mathbf{e}(\mathbf{z})_1(0) \\ -\mathbf{e}(\mathbf{z})_2(L) \end{bmatrix}, \quad Y\mathbf{e}(\mathbf{z}) = \begin{bmatrix} \mathbf{e}(\mathbf{z})_2(0) \\ \mathbf{e}(\mathbf{z})_1(L) \end{bmatrix}, \quad \mathbf{u} = \begin{bmatrix} p_0 \\ -m_L \end{bmatrix}.$$

Here, $\mathbf{e}(\mathbf{z})_i(x)$ denotes the i -th component of $\mathbf{e}(\mathbf{z})$, evaluated at x , i.e., for $x = 0$ and $x = L$, at the inflow and outflow of the pipe, respectively.

2.2 Compressor Model

Compressors are used in gas networks to increase gas pressure, which drops along pipes due to friction. The most commonly used compressors in gas networks are *centrifugal compressors* and *piston compressors*. While the internal physics of a compressor are quite complex, the relation between the *compression ratio*

$$\tilde{c} = \frac{p_{\text{out}}}{p_{\text{in}}}\tag{5}$$

and the *enthalpy* H_{ad} added to the gas is given by [12, 21]

$$H_{\text{ad}} = z(p_{\text{in}}, T_{\text{in}}) T_{\text{in}} R_s \frac{\kappa}{\kappa - 1} \left(\left(\frac{p_{\text{out}}}{p_{\text{in}}} \right)^{\frac{\kappa - 1}{\kappa}} - 1 \right),\tag{6}$$

where κ denotes the *isentropic exponent*. For a specific given compressor, the enthalpy H_{ad} is a function of the mass flow rate and the drive speed of the compressor, which is usually approximated from data.

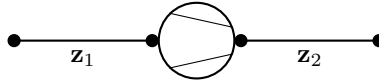


Figure 1: A compressor is inserted between two pipes.

To insert a compressor between two pipes in a port-Hamiltonian framework, we combine two pipes from (4), visualized in Fig. 1, and implement the compressor in the matrix $\hat{\mathbf{G}}(\hat{\mathbf{z}})$ and the boundary vector $\hat{\mathbf{u}}$ as

$$\begin{aligned}\hat{\mathbf{E}} \frac{\partial \hat{\mathbf{z}}}{\partial t} &= \left(\hat{\mathbf{J}}(\hat{\mathbf{z}}) - \hat{\mathbf{R}}(\hat{\mathbf{z}}) \right) \hat{\mathbf{e}}(\hat{\mathbf{z}}) + \hat{\mathbf{G}} \hat{\mathbf{u}} \\ \hat{\mathbf{y}} &= \hat{\mathbf{G}}^T \hat{\mathbf{e}}(\hat{\mathbf{z}}),\end{aligned}\tag{7}$$

where

$$\hat{\mathbf{z}} = \begin{bmatrix} \mathbf{z}_1 \\ \mathbf{z}_2 \end{bmatrix}, \quad \hat{\mathbf{e}}(\hat{\mathbf{z}}) = \begin{bmatrix} \mathbf{e}(\mathbf{z}_1) \\ Y\mathbf{e}(\mathbf{z}_1) \\ \mathbf{e}(\mathbf{z}_2) \\ Y\mathbf{e}(\mathbf{z}_2) \end{bmatrix},$$

$$\hat{\mathbf{E}} = \begin{bmatrix} I_2 & 0 \\ 0 & 0 \\ 0 & I_2 \\ 0 & 0 \end{bmatrix}, \quad \hat{\mathbf{J}}(\hat{\mathbf{z}}) = \begin{bmatrix} \mathbf{J}_1(\mathbf{z}_1) & 0 & 0 & 0 \\ -U & 0 & 0 & 0 \\ 0 & 0 & \mathbf{J}_2(\mathbf{z}_2) & 0 \\ 0 & 0 & -U & 0 \end{bmatrix}, \quad \hat{\mathbf{R}}(\hat{\mathbf{z}}) = \begin{bmatrix} \mathbf{R}_1(\mathbf{z}_1) & 0 & 0 & 0 \\ 0 & 0 & 0 & 0 \\ 0 & 0 & \mathbf{R}_2(\mathbf{z}_2) & 0 \\ 0 & 0 & 0 & 0 \end{bmatrix}.$$

We model compressors as jump conditions under two different assumptions and in two different frameworks, respectively.

1. **Assumption AV:** Constant velocity of the gas is assumed across the compressor, as in [5, Table 9.2]. In this case, the relationship between the momentum m_{in} at the inlet of the compressor and the momentum m_{out} at the outlet is given by

$$m_{\text{out}} = \tilde{c}^{\frac{1}{\kappa}} \frac{z(p_{\text{in}}, T_{\text{in}})}{z(p_{\text{out}}, T_{\text{out}})} m_{\text{in}}. \quad (\text{AV})$$

In practice, we consider z to be constant, so that we model $m_{\text{out}} = \tilde{c}^{\frac{1}{\kappa}} m_{\text{in}}$.

2. **Assumption AM:** Constant momentum of the gas is assumed across the compressor, as in [12, 19, 22]. In this case

$$m_{\text{out}} = m_{\text{in}}. \quad (\text{AM})$$

Under both of those assumptions, we model compressors in the following two frameworks.

2.2.1 Framework FC

We choose the compression ratio \tilde{c} of the compressor, meaning the output pressure varies with the input pressure

$$p_{\text{out}}(\tilde{c}, p_{\text{in}}) = \tilde{c} p_{\text{in}}. \quad (\text{FC})$$

In this case, the matrix $\hat{\mathbf{G}}(\hat{\mathbf{z}})$ in (7) is given by

$$\hat{\mathbf{G}}_{\text{FC}}(\hat{\mathbf{z}}) = \begin{bmatrix} 0 & 0 & 0 & 0 \\ 1 & 0 & 0 & 0 \\ 0 & -m_2(0) & 0 & 0 \\ 0 & 0 & 0 & 0 \\ 0 & 0 & p_1(L) & 0 \\ 0 & 0 & 0 & 1 \end{bmatrix},$$

and, depending on the assumption, the boundary vector $\hat{\mathbf{u}}$ is given by

$$\hat{\mathbf{u}}_{\text{FC}}^{\text{AV}} = \begin{bmatrix} p_0 \\ \tilde{c}^{-\frac{1}{\kappa}} \\ \tilde{c} \\ -m_L \end{bmatrix} \quad \text{or} \quad \hat{\mathbf{u}}_{\text{FC}}^{\text{AM}} = \begin{bmatrix} p_0 \\ 1 \\ \tilde{c} \\ -m_L \end{bmatrix}.$$

The output $\hat{\mathbf{y}}$ in this setting is given by

$$\hat{\mathbf{y}}_{\text{FC}}(\hat{\mathbf{z}}) = \hat{\mathbf{G}}_{\text{FC}}(\hat{\mathbf{z}})^T \hat{\mathbf{e}}(\hat{\mathbf{z}}) = \begin{bmatrix} m_1(0) \\ -m_2(0)p_1(L) \\ p_1(L)m_2(0) \\ p_2(L) \end{bmatrix},$$

which leads to external energy exchange

$$\begin{aligned}\hat{\mathbf{y}}_{\text{FC}}(\hat{\mathbf{z}})^T \hat{\mathbf{u}}_{\text{FC}}^{\text{AV}} &= p_1(0)m_1(0) - p_2(L)m_2(L) + \left(\tilde{c} - \tilde{c}^{-\frac{1}{\kappa}}\right) p_1(L)m_2(0), \text{ or} \\ \hat{\mathbf{y}}_{\text{FC}}(\hat{\mathbf{z}})^T \hat{\mathbf{u}}_{\text{FC}}^{\text{AM}} &= p_1(0)m_1(0) - p_2(L)m_2(L) + (\tilde{c} - 1) p_1(L)m_2(0).\end{aligned}$$

In both cases, we see that for compression ratio $\tilde{c} = 1$, the external energy exchange is the energy inserted at the inlet minus the energy removed at the outlet, while for a compression ratio $\tilde{c} > 1$, energy is added by the compressor.

2.2.2 Framework FP

We choose the output pressure p_{out} of the compressor, meaning the compression ratio varies depending on the input pressure

$$\tilde{c}(p_{\text{out}}, p_{\text{in}}) = \frac{p_{\text{out}}}{p_{\text{in}}}. \quad (\text{FP})$$

In this case, depending on the assumption, the matrix $\hat{\mathbf{G}}(\hat{\mathbf{z}})$ in (7) is given by

$$\hat{\mathbf{G}}_{\text{FP}}^{\text{AV}}(\hat{\mathbf{z}}) = \begin{bmatrix} 0 & 0 & 0 & 0 \\ 1 & 0 & 0 & 0 \\ 0 & -m_2(0)p_1(L)^{\frac{1}{\kappa}} & 0 & 0 \\ 0 & 0 & 0 & 0 \\ 0 & 0 & 1 & 0 \\ 0 & 0 & 0 & 1 \end{bmatrix} \quad \text{or} \quad \hat{\mathbf{G}}_{\text{FP}}^{\text{AM}}(\hat{\mathbf{z}}) = \begin{bmatrix} 0 & 0 & 0 & 0 \\ 1 & 0 & 0 & 0 \\ 0 & -m_2(0) & 0 & 0 \\ 0 & 0 & 0 & 0 \\ 0 & 0 & 1 & 0 \\ 0 & 0 & 0 & 1 \end{bmatrix}$$

and, depending on the assumption, the boundary vector $\hat{\mathbf{u}}$ is given by

$$\hat{\mathbf{u}}_{\text{FP}}^{\text{AV}} = \begin{bmatrix} p_0 \\ -\frac{1}{\kappa} \\ p_{\text{out}} \\ p_{\text{out}} \\ -m_L \end{bmatrix} \quad \text{or} \quad \hat{\mathbf{u}}_{\text{FP}}^{\text{AM}} = \begin{bmatrix} p_0 \\ 1 \\ p_{\text{out}} \\ -m_L \end{bmatrix}.$$

The output $\hat{\mathbf{y}}$ in this setting, depending on the assumption, is given by

$$\hat{\mathbf{y}}_{\text{FP}}^{\text{AV}}(\hat{\mathbf{z}}) = \hat{\mathbf{G}}_{\text{FP}}^{\text{AV}}(\hat{\mathbf{z}})^T \hat{\mathbf{e}}(\hat{\mathbf{z}}) = \begin{bmatrix} m_1(0) \\ -m_2(0)p_1(L)^{\frac{\kappa+1}{\kappa}} \\ m_2(0) \\ p_2(L) \end{bmatrix} \quad \text{or} \quad \hat{\mathbf{y}}_{\text{FP}}^{\text{AM}}(\hat{\mathbf{z}}) = \hat{\mathbf{G}}_{\text{FP}}^{\text{AM}}(\hat{\mathbf{z}})^T \hat{\mathbf{e}}(\hat{\mathbf{z}}) = \begin{bmatrix} m_1(0) \\ -m_2(0)p_1(L) \\ m_2(0) \\ p_2(L) \end{bmatrix}$$

which leads to external energy exchange

$$\begin{aligned}\hat{\mathbf{y}}_{\text{FP}}^{\text{AV}}(\hat{\mathbf{z}})^T \hat{\mathbf{u}}_{\text{FP}}^{\text{AV}} &= p_1(0)m_1(0) - p_2(L)m_2(L) + \left(p_{\text{out}} - p_1(L) \left(\frac{p_1(L)}{p_{\text{out}}}\right)^{\frac{1}{\kappa}}\right) m_2(0), \text{ or} \\ \hat{\mathbf{y}}_{\text{FP}}^{\text{AM}}(\hat{\mathbf{z}})^T \hat{\mathbf{u}}_{\text{FP}}^{\text{AM}} &= p_1(0)m_1(0) - p_2(L)m_2(L) + (p_{\text{out}} - p_1(L)) m_2(0).\end{aligned}$$

In both cases, it is readily seen that if the pressure at the inlet of the compressor $p_1(L)$ is equal to the output pressure p_{out} , no energy is added by the compressor.

2.3 Network Interconnection

Structure preserving interconnection of the compressor model into a port-Hamiltonian gas network can be done by extension of the approach in [15, Section 10.2], i.e., by implementing a third incidence matrix A_C for the compressor nodes, in addition to the incidence matrices for the internal nodes A_I and boundary nodes A_B .

Accordingly, all the port-Hamiltonian pipes and compressors in a given network are stacked in block diagonal form into $\mathbf{E}(\mathbf{z})$, $\mathbf{J}(\mathbf{z})$, $\mathbf{R}(\mathbf{z})$ and $\mathbf{G}(\mathbf{z})$. Assuming that the nodes are ordered in such a way that the first set of nodes are the boundary nodes, the second set of nodes — the compressor

nodes, and the third set of nodes — the internal nodes. Thus, the dynamics of the system are then given by

$$\begin{bmatrix} \mathbf{E}(\mathbf{z}) & 0 & 0 & 0 & 0 \\ 0 & 0 & 0 & 0 & 0 \\ 0 & 0 & 0 & 0 & 0 \\ 0 & 0 & 0 & 0 & 0 \\ 0 & 0 & 0 & 0 & 0 \end{bmatrix} \begin{bmatrix} \dot{\mathbf{z}} \\ \dot{\mu} \\ \dot{\lambda}_B \\ \dot{\lambda}_C \\ \dot{\lambda}_I \end{bmatrix} = \begin{bmatrix} \mathbf{J}(\mathbf{z}) - \mathbf{R}(\mathbf{z}) & \mathbf{G}(\mathbf{z}) & 0 & 0 & 0 \\ -\mathbf{G}(\mathbf{z})^T & 0 & A_B^T & A_C^T & A_I^T \\ 0 & -A_B & 0 & 0 & 0 \\ 0 & -A_C & 0 & 0 & 0 \\ 0 & -A_I & 0 & 0 & 0 \end{bmatrix} \begin{bmatrix} \mathbf{e}(\mathbf{z}) \\ \mu \\ \lambda_B \\ \lambda_C \\ \lambda_I \end{bmatrix} + \begin{bmatrix} 0 & 0 \\ 0 & 0 \\ I_b & 0 \\ 0 & I_c \\ 0 & 0 \end{bmatrix} \begin{bmatrix} \mathbf{u}_B \\ \mathbf{u}_C \end{bmatrix}$$

$$\mathbf{y} = \begin{bmatrix} 0 & 0 & I_b & 0 & 0 \\ 0 & 0 & 0 & I_c & 0 \end{bmatrix} \begin{bmatrix} \mathbf{e}(\mathbf{z}) \\ \mu \\ \lambda_B \\ \lambda_C \\ \lambda_I \end{bmatrix} = \begin{bmatrix} \lambda_B \\ \lambda_C \end{bmatrix}. \quad (8)$$

Example In case of the simple network depicted in Fig. 2, the incidence matrices are

$$A_B = \begin{bmatrix} 1 & 0 & 0 & 0 & 0 & 0 & 0 & 0 \\ 0 & 0 & 0 & 0 & 0 & 1 & 0 & 0 \\ 0 & 0 & 0 & 0 & 0 & 0 & 0 & 1 \end{bmatrix},$$

$$A_C = \begin{bmatrix} 0 & 1 & 0 & 0 & 0 & 0 & 0 & 0 \\ 0 & 0 & 1 & 0 & 0 & 0 & 0 & 0 \end{bmatrix} \text{ and}$$

$$A_I = [0 \ 0 \ 0 \ 1 \ 1 \ 0 \ 1 \ 0].$$

The boundary inputs are given as $\mathbf{u}_B = \begin{bmatrix} p_{\text{in}}^{\mathbf{v}_1} \\ -m_{\text{out}}^{\mathbf{v}_2} \\ -m_{\text{out}}^{\mathbf{v}_3} \end{bmatrix}$, where $p_{\text{in}}^{\mathbf{v}_1}$ is the inlet pressure at \mathbf{v}_1 and

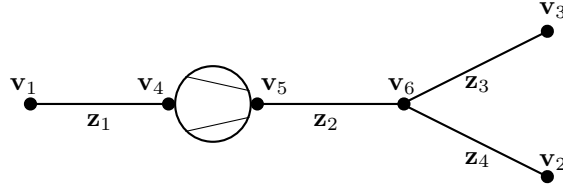


Figure 2: A simple pipe network with an inserted compressor.

$m_{\text{out}}^{\mathbf{v}_i}$ are the outlet momenta at \mathbf{v}_i , $i = 1, 2$. The inputs for the compressor, \mathbf{u}_C , are, according to assumption **AV** and framework **FC**,

$$\mathbf{u}_C^{\text{AV,FC}} = \begin{bmatrix} \tilde{c}^{-\frac{1}{\kappa}} \\ \tilde{c} \end{bmatrix}, \quad \mathbf{u}_C^{\text{AM,FC}} = \begin{bmatrix} 1 \\ \tilde{c} \end{bmatrix}, \quad \mathbf{u}_C^{\text{AV,FP}} = \begin{bmatrix} -\frac{1}{\kappa} \\ p_{\text{out}} \end{bmatrix} \quad \text{and} \quad \mathbf{u}_C^{\text{AM,FP}} = \begin{bmatrix} 1 \\ p_{\text{out}} \end{bmatrix}.$$

3 Numerical Experiments

As an indicative experiment, the widely benchmarked Yamal-Europe pipeline testcase is considered for its simplicity, similar to various articles in literature [3, 13]. The gas flow over a day is computed using the port-Hamiltonian model across the 363 km-long, 1.422 m-diameter pipeline with a minor modification. A compressor with a variable configuration is placed exactly midway along the pipeline (Fig 1). The gas is supplied into the left pipe consistently with a temperature of 276.25 K and pressure of 80 bar. A variable flow rate is chosen for gas extraction at the end of the right pipe at every 6 h period during the day. The pipe friction factor is considered a constant value of 1.8×10^{-3} . The fluid is considered ideal with a gas constant of $530 \text{ J kg}^{-1} \text{ mol}^{-1}$ and an isentropic exponent of 1.4.

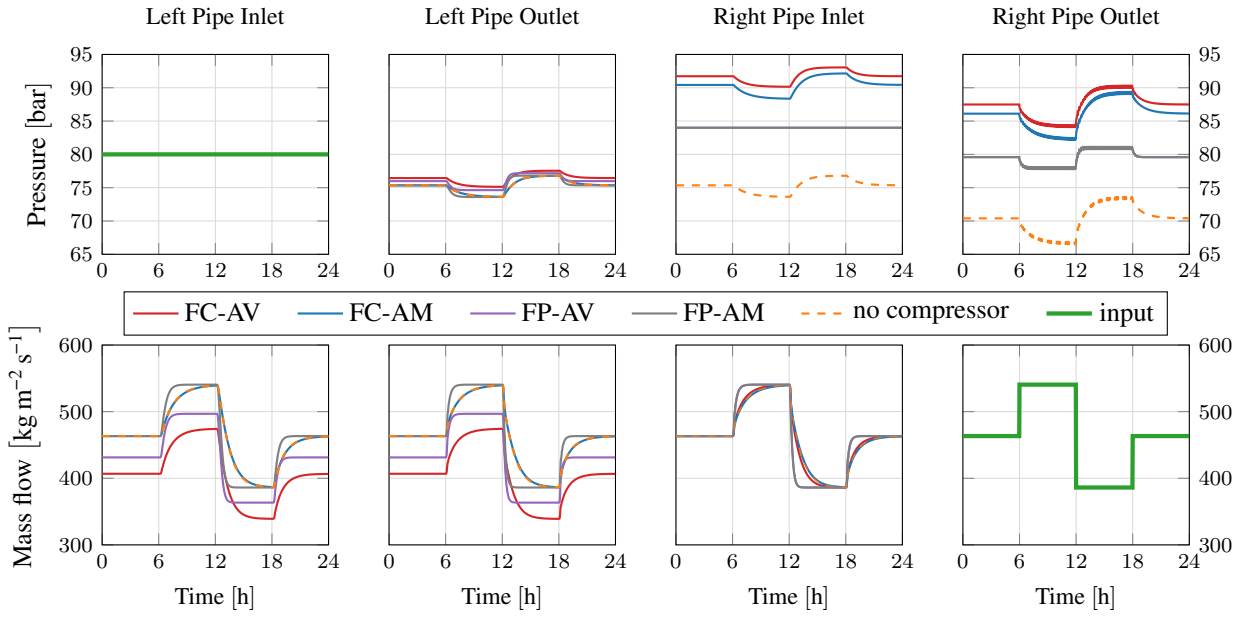


Figure 3: Pressure and Momentum values at each of the nodes for four different models of compressor placed between two pipes.

The numerical implementation of the model utilizes the finite difference method in space. The pipe is discretized in space into 32 equal intervals and a steady state simulation is performed for the initial boundary conditions ignoring the time-derivative terms in the port-Hamiltonian model to serve as initial conditions for the transient case. The transient simulation is subsequently computed for the dynamic discontinuous boundary conditions using an implicit-midpoint integration with a timestep of 100 s. The numerical scheme is particularly chosen for its numerical stability [15].

The simulation is performed for compressor models where the specified parameter is either compression ratio (FC) or output pressure (FP). For the FC framework, the compression ratio is 1.2, whereas for the FP framework, a constant compressor pressure of 84 bar is specified. The two different frameworks are paired with either a constant velocity assumption (AV) or a constant momentum assumption (AM). Fig 3 shows the result of pressure and momentum values at the inlet and outlet of the two pipes across the compressor. The results are contrasted against values obtained when there is no compressor present between the pipes. It is clearly observed that for FC compressors, the inlet pressure at the right pipe is scaled by the compression ratio factor relative to the outlet pressure at the left pipe. Additionally for FP compressors, the gas into the compressor maintains a fixed outlet pressure. The AM assumption ensures a constant momentum across the compressor while AV assumption allows variations. The choice of the right compressor model and assumption is seen to have significant effect on the pressure and momentum fields within the adjacent pipes.

4 Conclusion

The objective of this investigation was to explore the inclusion of compressor models in the port-Hamiltonian framework for gas networks. Four different models of compressors were considered with a pairwise combination of two specifications, either a compression ratio or output pressure; and two assumptions, constant velocity or constant momentum. The compressor models were imbued into an isothermal port-Hamiltonian model for gas networks by linking the nodes across it through ports. The numerical implementation of the model was performed and the results displayed the validity of the proposed model. The study serves as a preliminary outlook into developing an integrated energy-based model for gas networks.

Software Material

The scripts used in this article are developed using C++ programming language and containerized for reproducibility. Eigen library [7] is used to handle operators and linear algebra, and Ceres solver [1] is used to solve the system of non-linear equations. The record of the code along with execution instructions are available with doi:10.5281/zenodo.11387852 [16].

Acknowledgments

The authors thank Riccardo Morandin and Karim Cherifi for helpful discussions.

References

- [1] S. Agarwal, K. Mierle, et al. Ceres Solver, 2023. URL: <https://github.com/ceres-solver/ceres-solver>.
- [2] A. Bermúdez and M. Shabani. Modelling compressors, resistors and valves in finite element simulation of gas transmission networks. *Appl. Math. Model.*, 89:1316–1340, 2021. doi:10.1016/j.apm.2020.08.013.
- [3] M. Chaczykowski. Sensitivity of pipeline gas flow model to the selection of the equation of state. *Chemical Engineering Research and Design*, 87:1596–1603, 2009. doi:10.1016/j.cherd.2009.06.008.
- [4] P. Domschke, B. Hiller, J. Lang, V. Mehrmann, R. Morandin, and C. Tischendorf. Gas network modeling: An overview. Technical report, Technische Universität Darmstadt, 2021. Collaborative Research Center TRR 154. URL: <https://opus4.kobv.de/opus4-trr154>.
- [5] A. F. El-Sayed. *Fundamentals of Aircraft and Rocket Propulsion*, chapter Centrifugal and Axial Compressors, pages 703–838. Springer London, 2016. doi:10.1007/978-1-4471-6796-9_9.
- [6] S. A. Gorji. Challenges and opportunities in green hydrogen supply chain through meta-heuristic optimization. *Journal of Computational Design and Engineering*, 10(3):1143–1157, 05 2023. doi:10.1093/jcde/qwad043.
- [7] G. Guennebaud, B. Jacob, et al. Eigen, 2010. URL: <http://eigen.tuxfamily.org>.
- [8] V. Gyrya and A. Zlotnik. An explicit staggered-grid method for numerical simulation of large-scale natural gas pipeline networks. *Appl. Math. Model.*, 2019. doi:10.1016/j.apm.2018.07.051.
- [9] S. A. Hauschild and N. Marheineke. Extended group finite element method for a port-Hamiltonian formulation of the non-isothermal Euler equations. In *PAMM*. Wiley, 2021. doi:10.1002/pamm.202100032.
- [10] S. A. Hauschild and N. Marheineke. Structure-preserving discretization of a port-Hamiltonian formulation of the non-isothermal Euler equations. In *PAMM*. Wiley, 2021. doi:10.1002/pamm.202000014.
- [11] S. A. Hauschild and N. Marheineke. Structure-preserving methods for a coupled port-Hamiltonian system of compressible non-isothermal fluid flow. In *PAMM*. Wiley, 2023. doi:10.1002/pamm.202300012.
- [12] M. Herty. Modeling, simulation and optimization of gas networks with compressors. *Netw. Heterog. Media*, 2(1):81–97, 2007. doi:10.3934/nhm.2007.2.81.
- [13] C. Himpe, S. Grundel, and P. Benner. Model order reduction for gas and energy networks. *J. Math. Ind.*, 11(1), July 2021. doi:10.1186/s13362-021-00109-4.

- [14] M. W. Melaina, O. Antonia, and M. Penev. Blending hydrogen into natural gas pipeline networks: A review of key issues. Technical report, National Renewable Energy Laboratory, 2013. NREL/TP-5600-51995. URL: <https://www.osti.gov/biblio/1068610>, doi: [10.2172/1068610](https://doi.org/10.2172/1068610).
- [15] R. Morandin. *Modeling and numerical treatment of port-Hamiltonian descriptor systems*. PhD thesis, Technische Universität Berlin, January 2024. doi:<https://doi.org/10.14279/depositonce-19826>.
- [16] A. S. Nayak and T. Bendokat. phgasnets: Code supplement for article "Modelling Gas Networks with Compressors: A Port-Hamiltonian Approach", 2024. doi:[10.5281/zenodo.11387852](https://doi.org/10.5281/zenodo.11387852).
- [17] K. A. Pambour, R. Bolado-Lavin, and G. P. J. Dijkema. An integrated transient model for simulating the operation of natural gas transport systems. *J. Nat. Gas Sci. Eng.*, 28:672–690, 2016. doi:[10.1016/j.jngse.2015.11.036](https://doi.org/10.1016/j.jngse.2015.11.036).
- [18] M. A. Semeraro. Renewable energy transport via hydrogen pipelines and hvdc transmission lines. *Energy Strategy Reviews*, 35:100658, 2021. doi:[10.1016/j.esr.2021.100658](https://doi.org/10.1016/j.esr.2021.100658).
- [19] K. Sundar and A. Zlotnik. State and parameter estimation for natural gas pipeline networks using transient state data. *IEEE Trans. Control Syst. Technol.*, 27(5):2110–2124, 2019. doi: [10.1109/tcst.2018.2851507](https://doi.org/10.1109/tcst.2018.2851507).
- [20] A. J. van der Schaft and D. Jeltsema. Port-hamiltonian systems theory: An introductory overview. *Foundations and Trends[®] in Systems and Control*, 1(2):173–378, 2014. doi:[10.1561/2600000002](https://doi.org/10.1561/2600000002).
- [21] T. Walther and B. Hiller. Modelling compressor stations in gas networks. Technical report, Zuse Institute Berlin, 2017. URL: <https://nbn-resolving.org/urn:nbn:de:0297-zib-67443>.
- [22] A. Zlotnik, M. Chertkov, and S. Backhaus. Optimal control of transient flow in natural gas networks. In *2015 54th IEEE Conference on Decision and Control (CDC)*, pages 4563–4570. IEEE, 2015. doi:[10.1109/CDC.2015.7402932](https://doi.org/10.1109/CDC.2015.7402932).